RSC Advances

ROYAL SOCIETY OF CHEMISTRY

www.rsc.org/advances

Graphical abstract

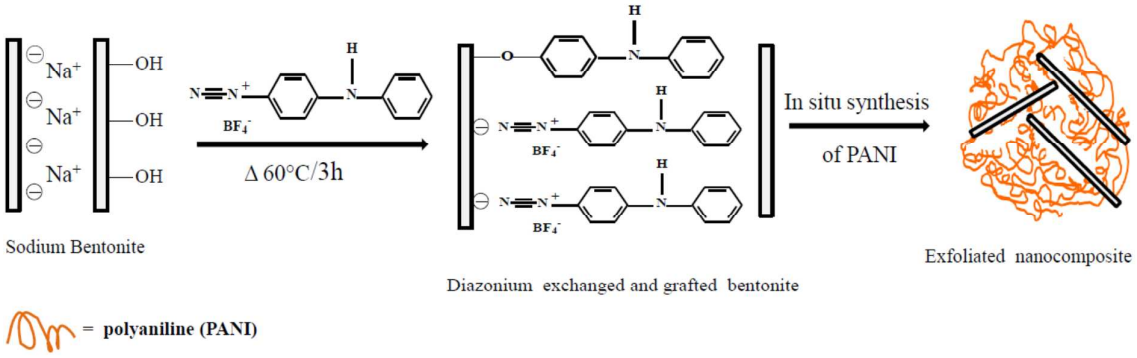

Exfoliated, conductive clay/polyaniline nanocomposites were prepared by polymerization of aniline in the presence of diazonium cation exchanged bentonite.

Exfoliated clay/polyaniline nanocomposites through tandem diazonium cation exchange reactions and in-situ oxidative polymerization of aniline

Khouloud Jlassi[1,2,3], *Ahmed Mekki*[3,4], *Mémia Benna-Zayani*[1,2], *Ajay Singh*[5], *Dinesh K. Aswal*[5], *Mohamed M. Chehimi*[3,6]

[1] *Université de Carthage, Faculté des Sciences de Bizerte (FSB), LACReSNE, Bizerte, Tunisia.*
[2] *Institut Supérieur des Sciences et Technologies de l'Environnement (ISSTE), Borj Cédria, Tunisia.*
[3] *Univ Paris Diderot, Sorbonne Paris Cité, ITODYS, UMR CNRS 7086, 15 rue JA De Baïf, France.*
[4] *Ecole Militaire Polytechnique, BP 17, Bordj El Bahri 16111, Algiers, Algeria.*
[5] *Technical Physics Division, Bhabha Atomic Research Centre (BARC), Mumbai 400085, India*
[6] *Université Paris Est, ICMPE, SPC, PoPI team, UPEC, 2-8 rue Henri Dunant, 94320 Thiais, France.*

Abstract

Robust, conductive clay/polyaniline nanocomposites were prepared through a simple approach which consists of in-situ polymerizing aniline, in the presence of the 4-diphenylamine diazonium-modified bentonite. XPS measurements indicate that clay experiences a cation exchange of sodium by the diazonium, and the polyaniline is richly present at the nanocomposite surface. As judged by XRD, the clay basal distance increased from 13.7 to 16.2 Å after diazonium modification, whilst, after the in-situ polymerization of aniline, the clay characteristic peak at low angle (< 8°) has vanished evidencing the exfoliation of the resulting nanocomposites. However, the nanocomposite prepared with unmodified clay was also found to be a polyaniline-rich surface but without any sign of exfoliation. In addition, the composite morphology, imaged by electron microscopy (SEM) and (TEM), differs significantly from that of pristine clay and shows twisted layers with an inter-distance which increases with the mass loading of the diazonium salt and PANI therefore leading to the exfoliation of the clay. Furthermore, this diazonium modification resulted in a quantum jump of conductivity of the nanocomposites compared to bentonite, c.a. 6 orders of magnitude, whereas the deposition of PANI on pristine clay induced a marginal increase of conductivity from 10^{-9} to $2x10^{-8}$ S/cm due to an uneven coating of the conjugated polymer.

Keywords: Clay, diazonium salts, polyaniline, nanocomposites.

***corresponding authors:**
Mohamed M. Chehimi, chehimi@icmpe.cnrs.fr
Mémia Benna-Zayani, memia.benna@fsb.rnu.tn

Graphical abstract

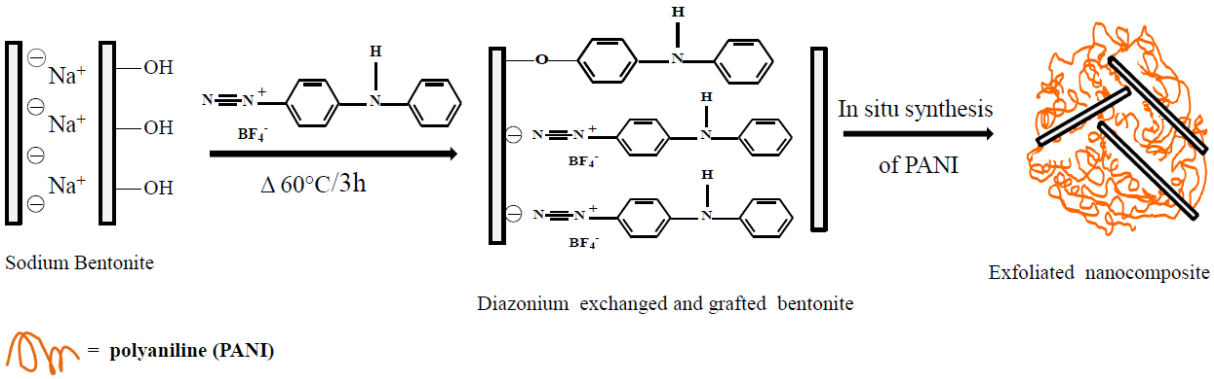

Exfoliated, conductive clay/polyaniline nanocomposites were prepared by polymerization of aniline in the presence of diazonium cation exchanged bentonite.

1. Introduction

The surface and interface chemistry of aryl diazonium salts is very well documented. [1,2,3,4] It has progressed at a remarkable pace in the last quarter a century since the pioneering work of Jean Pinson and co-workers in 1992 who described the mechanisms of attachment of aryl layers to glassy carbon electrodes by electroreduction of the parent diazonium salts. [5] Since then, much has been said about the applications of aryl diazonium salts in view of modifying the surface of sp2 carbons,[6] diamonds,[7,8,9] semi-conductors[10,11] and even insulating materials such as polymers,[12] glass[13] and silica nanoparticles[14] to name but a few. Of relevance to the actual paper, aryl layers from diazonium salts permit to bind thin polymer layers to materials surfaces by either *grafting to* or *grafting from* routes.[15] The latter served to graft either insulating polymethacrylates[15] or conductive, conjugated films such as poly (3,4-ethylenedioxythiophene)[16] or polyaniline (PANI).[17,18] For example, the diazotized 4-aminodiphenylaniline served for the modification of glassy carbon electrodes[17] and multiwalled carbon nanotubes[18] by aryl layers followed by graft polymerization of aniline. However, despite such remarkable advances in the surface and interface chemistry of aryl diazonium salts, only recently they have been used to modify layered silicates (clays).[19,20] On the one hand, Dabbagh *et al*.[19] employed clay catalyst for in-situ generation of aryl diazonium salts which further served for diazo coupling reations toward the synthesis of azo dyes. On the other hand Salmi *et al*.[20] designed a diazonium salt bearing dimethylamino group which efficiently initiated radical photopolymerization of glycidyl methacrylate within the confined interlamellar spacing of the clay. Interestingly, isolated diazonium salts react readily and efficiently with clays inducing swelling, visible with the naked eye.[20] Such a swelling is due to fast cation exchange reactions between the diazonium and sodium from the clay.

In our quest of new routes for clay/polymer nanocomposites, we shall consider the in-situ polymerization of conjugated monomers such as aniline. Clay/conjugated polymer

nanocomposites have made the subject of numerous reports and were found to be remarkable materials for anticorrosion coatings,[21] electrorheology,[22] catalysis,[23] electrochromic devices, [24] and other applications summarized by Omastová and Mičušík.[25] Polymerization of conjugated monomers can be conducted chemically[26] or by radiation-induced polymerization.[23] In the domain of surface science, it is of paramount importance to interrogate the propensity of surface modifiers and coupling agents to obtain nanocomposites with polymer-rich surfaces. This we have addressed with ammonium salts that impart hydrophobic properties to clays, a property that favors the formation of continuous conductive polymer layers.[26] Silanes have also been investigated in this regard.[27,28] Indeed, we have demonstrated that aminosilane-modified silica gel particles and glass slides are excellent hydrophobic substrates for the in-situ deposition of continuous, conductive polypyrrole layers. Recently, we used a silane functionalized with a pyrrolyl group to modify clay and showed that this group is an effective anchoring site for the in-situ formed polypyrrole/silver nanocomposite coating.[23]

In this work we shall bridge the gap between pretreatment of clay by diazonium salts and in-situ chemical polymerization of aniline. The diazonium salts provide anchor sites for the growing polyaniline (PANI). Such a strategy of making clay/polyaniline has never been envisaged with diazonium salts hence the motivation for our work.

The physicochemical properties of the resulting clay/PANI nanocomposites were characterized in terms of surface chemical composition by XPS, Raman, FTIR; morphology by SEM/TEM and XRD; we finished by determining the electrical conductivity of compressed pellets using the four probe technique.

2.Experimental

2.1. Reagents

The raw clay was extracted from the Gafsa-Metlaoui basin (Tunisia; the longitude, Lambert coordinates is about 6 grads and 69 minutes (east) and the latitude of 38 degrees and 27 minutes North). The clay was purified according to standard procedure described in references[29,30] in order to obtain the final ~80µm-sized soda clay (B-Na) particles. The cationic exchange capacity (CEC) of the clay was assessed by the well-known approach devised by Hang *et al.*[31] using methylene blue and found to be equal to 101.86meq/100 g of clay.

N-phenyl-p-phenylenediamine (Acros, 98% purity), isopentyl nitrite (Alfa Aesar, purity 97%), ammonium persulfate (APS, Acros, 98% purity) and nitric acid (Carlo Erba, 60% purity) were used as received. Aniline (Aldrich, 99.5% pure) was purified by passing it through a column of basic alumina powder (Merck, size ~ 63 µm) and then stored at low temperature prior to use. Deionized water was used throughout all experiments for synthesis and cleaning purposes.

2.2. Synthesis of 4-diphenylamine diazonium tetrafluoroborate

The synthesis of the 4-diphenylamine diazonium tetrafluoroborate was performed following standard procedure. Basically, N-phenyl-p-phenylenediamine (0.46 g, 2.5 mmol) was dissolved in 3 ml of acetone, cooled in an ice bath and subsequently 2 ml of HBF_4 (aqueous solution 48 v/v%) was added. Isopentyl nitrite (0.63g, 5.5mmol) was added drop-wise to the mixture which was kept under stirring for 10min. The final diazonium salt was left to decant overnight in the fridge and the crystallized precipitate was filtered and washed with copious amounts of cold ether.

2.3. Diazonium-modification of bentonite

To an aqueous suspension of clay (1g dissolved in 100 ml of de-ionized water) we added dropwise an aqueous solution of diazonium salt: 0.15, 0.3 and 0.45g in 30 ml of de-ionized water, which corresponds to 0.6, 1.3 and 2 times the clay cation exchange capacity (CEC). It is to note that upon addition of the diazonium solution, we systematically observed swelling of the clay as reported by Salmi *et al.*[20] The diazonium-modified clays were washed several times with water until the washings were clear, dried and then refluxed in acetonitrile for 3h at 60°C. This second purification step served for the removal of any loosely bound organics. Finally, the product was dried at 60°C. In the following sections, the 4-diphenylamine-modified clay is noted B-DPA_x (*x* stands for the CEC fraction) and purified bentonite is noted B.

2.4. Synthesis of clay/PANI nanocomposites

In all synthesis molar ratio of aniline/ammonium persulfate was taken at 4. In a typical procedure, a B-DPA_x sample (about 8 mg, corresponding to 7.52 mg of pure bentonite) was dispersed in 10 ml of acetonitrile and kept under ultrasonication for 5 min. The anilinium cation was prepared by mixing aniline (154.5 mg, 0.16 mol/L) with (291.5 mg, 0.32 mol/L) nitric acid. The mixture was left under magnetic stirring for 1 h. The desired amount of B-DPA was added to the anilinium cation solution maintained at low temperature using ice bath. The solution was stirred for more than 2h. Thereafter, aqueous solution of APS (91.3 mg, 0.04 mol/l in water) was added dropwise using a micropipette. The suspension was kept under ultrasonication for 5 min and then with constant stirring for more than 1h to allow the oxidative polymerization to proceed. The suspension turned to blue-greenish color after about 8 min from adding APS. The clay/PANI nanocomposite was filtered and washed sequentially with copious amounts of methanol and de-ionized water to remove un-reacted aniline and

oxidant. The final product was dried in oven at 60°C over night. The same protocol was followed to prepare the other clay/PANI nanocomposites using B-DPA with different CEC fractions (i.e. 0.6, 1.3 and 2). The nanocomposites are noted B-DPA$_x$/PANI where *x* stands for the fraction of CEC (0.6, 1.3 or 2).

For comparison, and in order to interrogate the effect of the diazonium cation exchange on the final properties, a clay/PANI nanocomposite (noted B/PANI) was prepared under similar conditions using unmodified soda clay (7.5 mg).

2.5. Characterization

XPS spectra were recorded with a Thermo VG Scientific ESCALAB 250 spectrometer (East Grinstead, UK) equipped with a monochromatic Al Kα X-ray source (1486.6 eV and 500 µm spot size). The specimens were pressed against insulating double-sided adhesive tapes on sample holders and pumped overnight in the fast entry lock. The pass energy was set at 150 and 40 eV for the survey and the narrow scans, respectively. Charge compensation was achieved with an electron flood gun (kinetic energy = 4 eV, filament current = 3 A, emission current = 0.3 mA) operated in the presence of argon at a partial pressure of 2.10^{-8} mbar in the analysis chamber. The spectra were calibrated against the C–C/C–H C1s component set at 285 eV. The surface composition was determined from the XPS peak area and the corresponding Scofield sensitivity factors corrected for the analyzer transmission work function.

FTIR spectra of KBr compressed pellets were recorded with a Nicolet Magna 860 FTIR (Thermo-Electron) spectrometer in the 400 and 4000 cm^{-1} wave number range with a resolution of 4 cm^{-1} over 50 scans. The spectra were baseline-corrected with Omnic 6.1 software. Raman spectroscopy was carried out using Horiba Labram HR evolution; excitation was set at 633 nm from He-Ne Laser at room temperature.

XRD patterns were recorded using an Empyrean diffractometer Panalytical operating at 45kV and 40 mA, with a Cu anode (wave length Kalpha = 1,5419 Å). The configuration is as follows: the incident optical system is a convergent mirror, the sample is loaded in a 1mm diameter capillary spinner and a multi-channel detector is used. This experimental setup promotes the random crystallographic orientation of the particles (although anisotropic) and also permits to measure exactly the positions of the peaks, and therefore the interlayer distances.

Scanning electron micrographs (SEM) were taken with a Zeiss Supra mke apparatus and Jeol 100 CX-II served for recording transmission electron microscopy (TEM) images. For TEM imaging, clay/PANI nanocomposites were mixed with a resin prior to microtome sample cutting.

3. Results and discussion

3.1. Strategy of making clay/polyaniline via diazonium cation exchange reaction.

The nanocomposites were prepared by sequential diazonium cation exchange reaction of the clay and in situ oxidative polymerization of aniline. Figure 1 depicts the general approach for *(i)* intercalating the clay by the diazonium followed by thermally induced grafting of the aryl groups, and *(ii)* in situ polymerization of aniline. The diazonium salt interacts with the layered aluminosilicate in different manners as reported for silane chemistry.[32] Cation exchange is the first to occur at room temperature. After intercalation of the diazonium cation, a reaction with clay can also lead to Si-O-N=N-C_6H_5 interfacial azoether group[19] which upon cure at 60°C yields –Si-O-C_6H_5 interfacial group. Azoethers are not stable and might even undergo dediazoniation at RT.[33] The mechanism of aniline polymerization within the clay is depicted

in Figure 1B. The polymerization process is very complex[34] and we retain here only the main reactions conducted in nitric acid using ammonium persulfate as oxidant.[35,36]

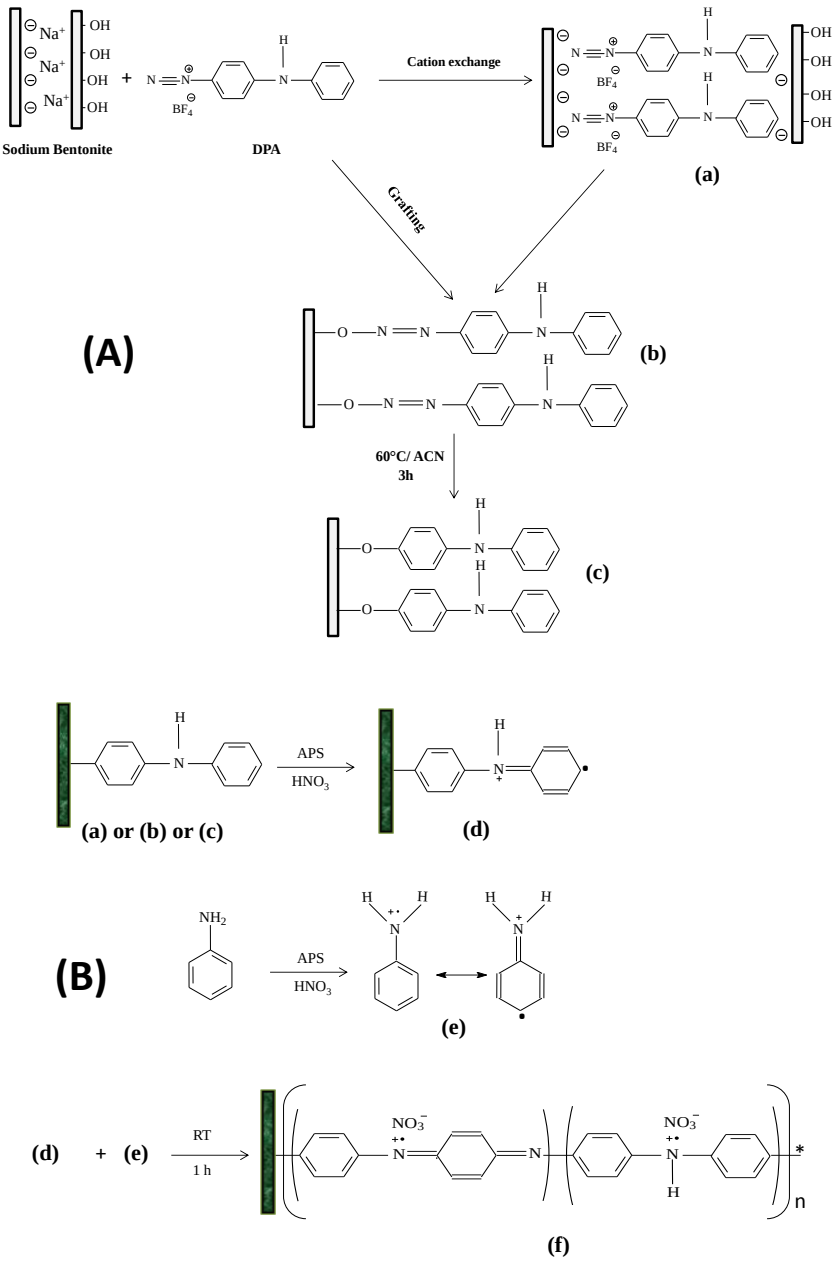

Figure 1. Chemical route for intercalating bentonite by diazonium cation exchange reaction and in situ polymerization (A, upper panel). Simplified mechanism of interfacial oxidative polymerization of aniline (B, lower panel).

3.2. Vibrational characterization by FTIR and Raman spectroscopies

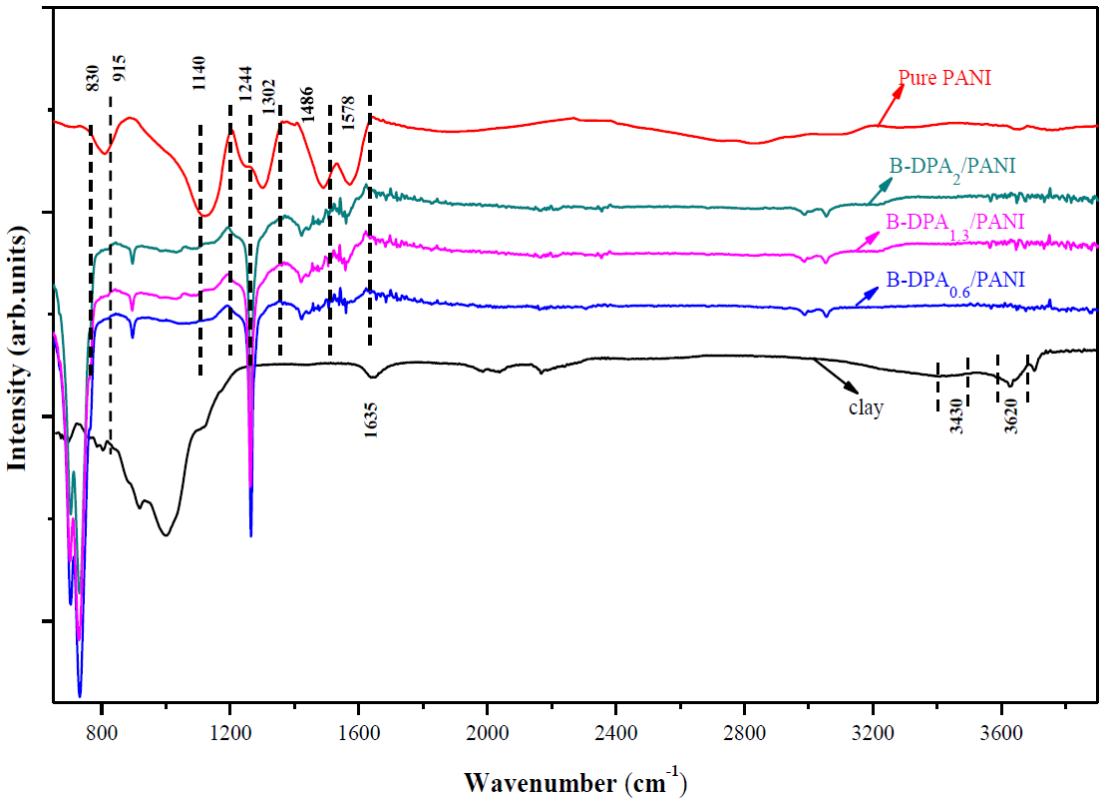

Figure 2. FTIR spectra of clay, PANI and B-DPA$_x$/PANI nanocomposites.

Recently, Stejskal and his team have employed UV-VIS, FITR and Raman spectroscopies to investigate polyaniline film growth on solid surface during in-situ polymerization of aniline.[37] The infrared bands centred at 3620 and 915 cm^{-1} confirm the dominant presence of dioctahedral smectite with [Al, Al-OH] stretching and bending bands.[38] The absorption bands at 3430 and 1635 cm^{-1} correspond to OH frequencies from the water molecule absorbed on the clay surface. The Si-O bands from the silicate structure have strong absorption bands at 1030 cm^{-1}. In the three B-DPA$_x$/PANI samples, the characteristics vibrations of bentonite are present in addition to the features from PANI centered at 1578, 1486, 1302, 1244 and 1140. The peak at 1302 cm^{-1} is due to π-electron delocalization induced in the polymer by protonation.[39,40] The peak at 1244 cm^{-1} is relative to C-N^{+} stretching vibrations in the

polaronic structure characterizing the conducting protonated form.[37] The spectra exhibit the bands at about 1578 and 1486 cm^{-1} assigned to C=C stretching of quinoid and benzenoid rings vibrations, respectively[41,42,43,44] indicating the oxidation state of PANI. In the FTIR spectra, a strong characteristic band appearing at 1140 cm^{-1} is ascribed to the ‘‘electron-like band’’ , it is considered to be a measure of the delocalization of the electrons and, thus, is indicative of the conductivity of PANI.[45,46] After coating of PANI on the clay-DPA, the spectrum reveals the presence of the polymer; the B-DPA_x/PANI spectra show nearly identical wave numbers 1578 and 1486 cm^{-1} assigned to quinoid and benzenoid ring at, respectively. Note however that the band at 1140 cm^{-1} is lumped with the broad Si-O-Si stretching peak of bentonite in the 1000-1200 cm^{-1} spectral range. Nevertheless, other peaks centred at 1587, 1486, 1302 and 1244 cm^{-1} testify to the presence of polyaniline in the nanocomposites.

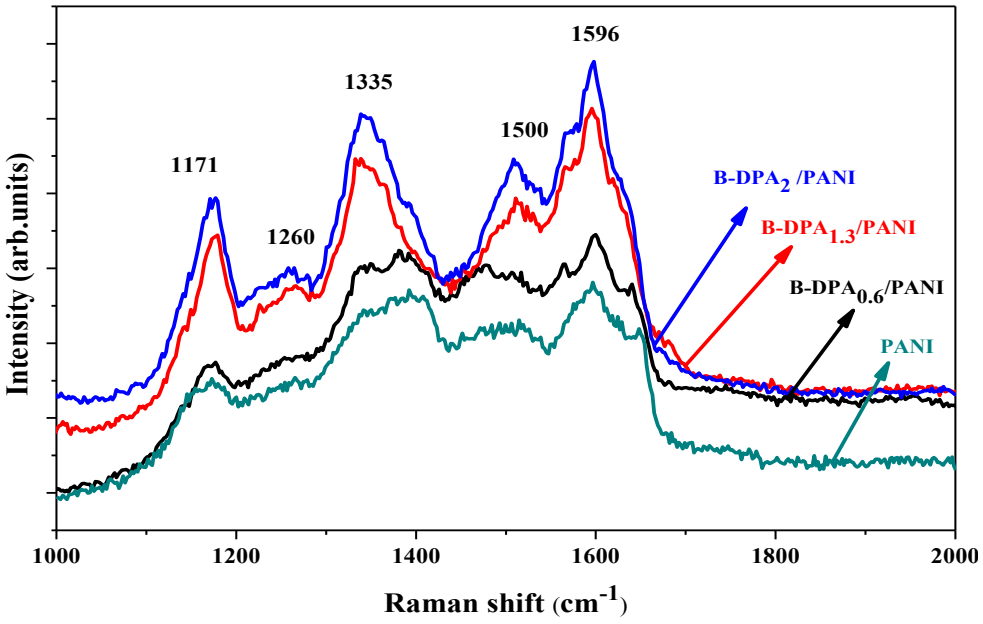

Figure 3. Raman spectra of bentonite/PANI nanocomposites.

The resonance Raman spectroscopy technique is sensitive to the electronic structure and vibrational properties of conducting polymers.[47] Typical Raman spectra of B-DPA_x/PANI

composites are shown in Figure 3. The typical bands of the doped polymer including C-H bending of the quinoid and benzenoid ring are centered at 1171 and 1260 cm^{-1}, respectively; C=N stretching of the quinoid ring at 1500 cm^{-1}, and C-C stretching of the quinoid rings at 1596 cm^{-1}. In the B-DPA_x/PANI samples, the characteristic vibrations are present in addition to the PANI features. B-DPA_x/PANI nanocomposites with a considerable cation exchange capacity such display intense bands at 1175 cm^{-1} suggesting the presence of more quinoid structure than the benzenoid in the PANI layer of composite samples. This may be due to the fact that the bentonite-DPA acts like a template for the directional polymerization of aniline and therefore enhancing the presence of more bipolaronic structure, which can consequently increases the number of quinoid units.

3.3. Surface analysis by means of XPS

The survey regions for the sodium clay (B-Na) before and after diazonium cation exchange followed by polymerization of aniline (B-DPA_2/PANI) are displayed in Figure 4. The main features are Al2p, Si2p, C1s, N1s, O1s and Na1s centred at ~74, 103, 285, 400, 532 and 1072 eV, respectively. Diazonium cation exchange is highlighted by a relatively intense C1s peak at 285 eV and particularly a depletion of the sodium peaks (Na1s at 1072 eV and the Auger NaKLL peak at ~492 eV. Indeed, sodium is stripped from clay and exchanged by the diazonium cation as we have observed recently for a diazonium salt bearing dimethylamino group.[20] The N1s peak from the diazonium salt is very small as the diazonium contains 1 N-H group per 12 carbon atoms. Nevertheless, one could track intercalation of the diazonium salt and its interactions with clay by examining the N1s region. Figure 5 displays the N1s region for B-DPA_2 before and after cure at 60 °C. In Figure 5a, the diazonium salt induces a complex N1s spectrum which has four components: the first one is assigned to C-N/N-H (~400 eV) whilst the second component at 402.7 eV is assigned to a protonated form of DPA. The

component centred at 403.4 eV is due to –N=N-O and N≡N$^+$-. The fourth component is centred at 406 eV and is assigned to the positively charged nitrogen atom of the diazonium N≡N$^+$-.[48] In Figure 5b, it is interesting to note the drastic change of the N1s peak shape. It reduces to two fitting components centred at 400 and 402.5 eV, assigned to free and protonated NH from DPA. The diazonium N1s peak at 406 eV has vanished and so the component due to azoether. After in-situ polymerization of aniline, the surface displays a survey region quasi identical to that of bulk powder PANI (not shown, see Table 1). Peaks from the underlying clay are not detected anymore at the exception of silicon. Survey spectra from all other nanocomposites are very comparable.

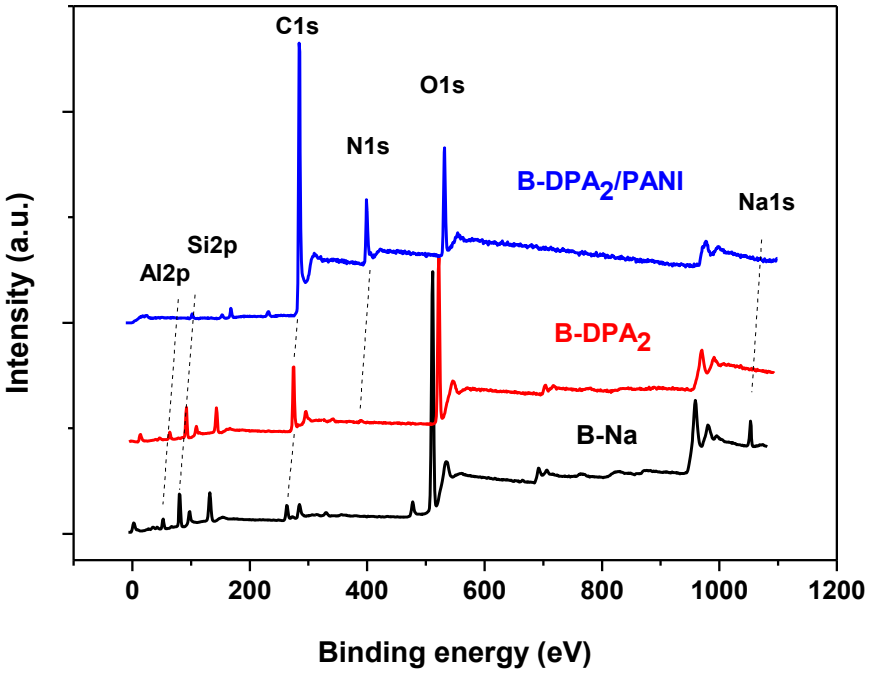

Figure 4. Survey spectra of sodium bentonite (B-Na), diazonium cation exchanged bentonite (B-DPA$_2$) and B-DPA$_2$/PANI nanocomposite.

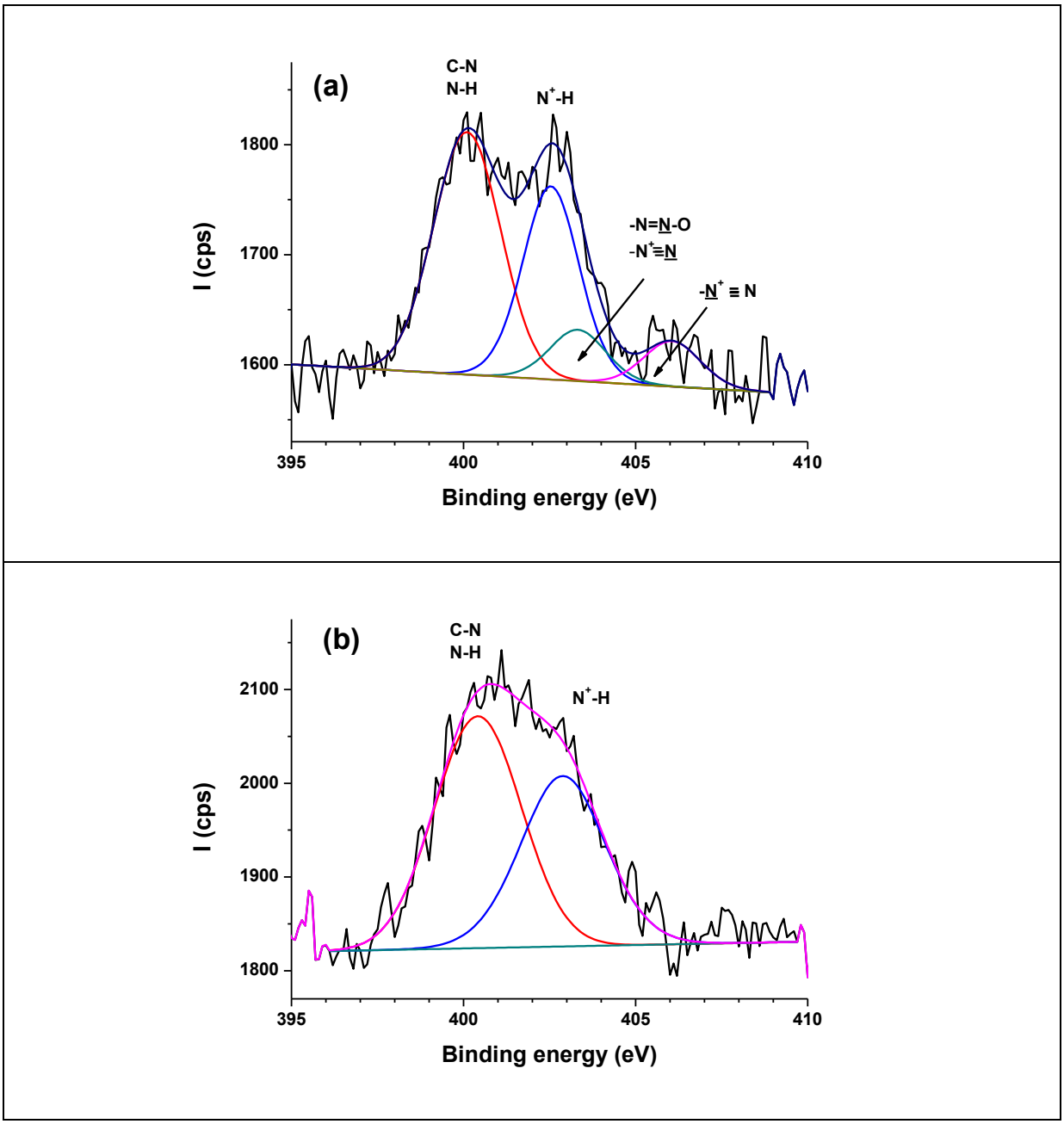

Figure 5. Peak fitted N1s region from B-DPA$_2$ (a) before, and (b) after cure at 60 °C.

The quantitative surface chemical compositions of the materials under test are reported in Table 1. Concerning the diazonium cation exchange, one can note a gradual increase of the carbon and nitrogen contents relative to those of elements from the underlying clay. As nitrogen and aluminum are unique elemental markers for the diazonium and the clay, respectively, we plotted N/Al atomic ratio versus the initial diazonium concentration expressed in CEC fraction (Figure 6). Saturation starts to be reached between 1.3 and 2 times the CEC. However, although a high CEC fraction induces higher diazonium loading, all nanocomposites reach almost a steady state composition and display comparable surface compositions as that of pure bulk powder PANI. This result means that PANI loading is high enough under all circumstances to permit a homogeneous coating of the clay lamellae.

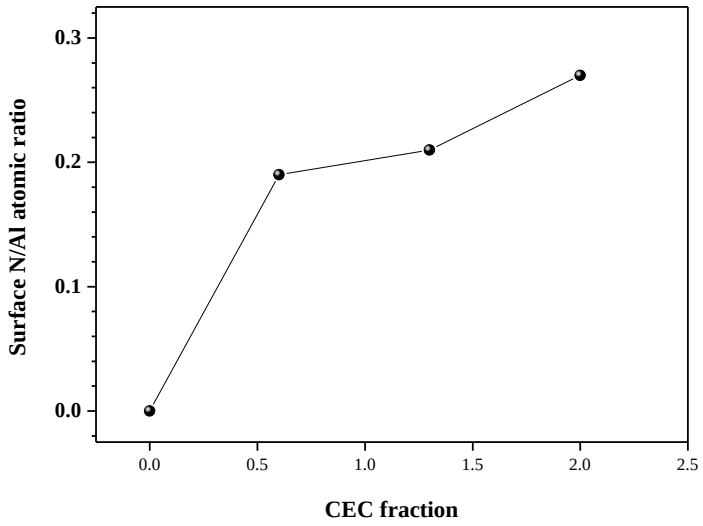

Figure 6. XPS-determined N/Al surface atomic ratio for B-Na and B-DPA versus the initial concentration of the diazonium salt expressed in CEC fraction.

Table 1. XPS-determined apparent surface composition of clay/PANI nanocomposites and reference materials.

Materials	**C**	**N**	**O**	**Si**	**Al**	**Na**	**K**	**Mg**
B-Na	6.82	-	63.4	19.1	8.15	0.71	0.61	1.23
B/PANI	80.9	9.90	9.07	0.17	-	-	-	-
B-DPA$_{0.6}$	14.2	1.37	54.4	20.7	7.20	0.13	0.44	1.52
B-DPA$_{0.6}$/PANI	79.9	10.7	9.29	0.11	-	-	-	-
B-DPA$_{1.3}$	19.3	1.50	50.5	20.2	7.18	0	0.38	1.03
B-DPA$_{1.3}$/PANI	77.9	10.5	10.7	0.91	-	-	-	-
B-DPA$_{2}$	29.5	1.65	44.7	16.8	6.09	0	0.25	1.03
B-DPA$_{2}$/PANI	76.4	9.62	10.7	1.39	-	-	-	-
Pure PANI	73.2	8.42	18.41	-	-	-	-	-

3.4. Scanning electron microscopy

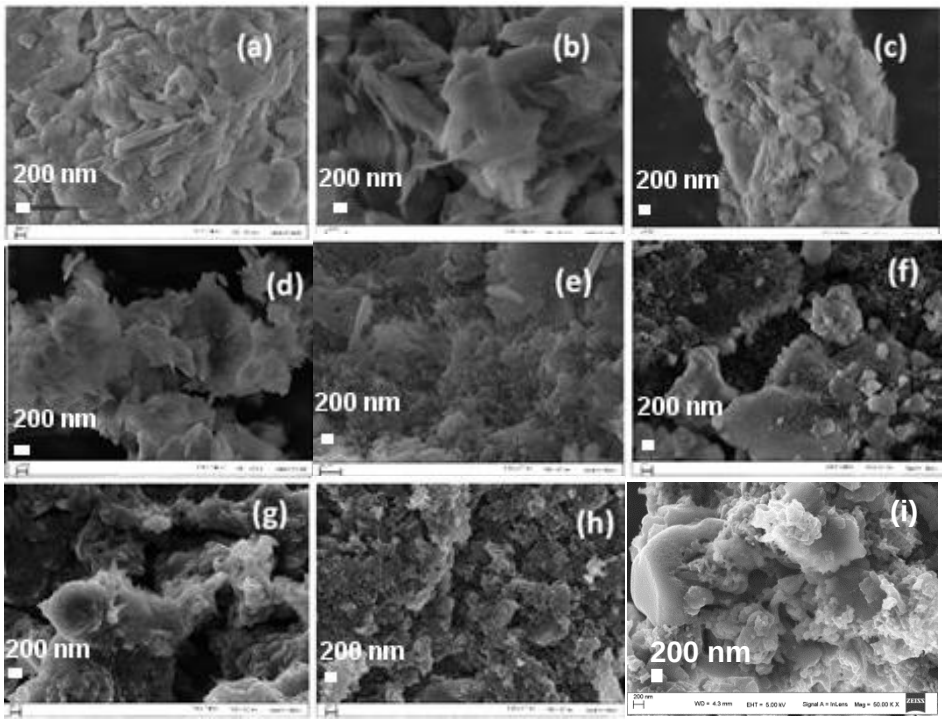

Figure 7. SEM images of (a) B-Na, (b) B-DPA$_{0.6}$, (c) B-DPA$_{1.3}$, (d) B-DPA$_2$, (e) PANI, (f) B-DPA$_{0.6}$/PANI, (g) B-DPA$_{1.3}$/PANI, (h) B-DPA$_2$/PANI, (i) B/PANI.

Figure 7 displays SEM pictures of pristine and modified clay samples. It shows that the surface modification of bentonite by the diazonium followed by grafting PANI induces remarkable alterations of the clay morphology. It can be seen that pristine bentonite exhibits compact grain morphology (Figure 7a) which gradually changes due to progressive intercalation by the diazonium salts (Figures 7b-d). Pure PANI sample exhibits a granular morphology (Figure 7e), while the bentonite-PANI nanocomposite displays a homogenous structure that differs markedly from that of neat bentonite (Figures 7f-h). Moreover, there is no presence of granular PANI which suggests that PANI coating occurs on both the surface layers and the interlayer space. Additionally, for the nanocomposite B-DPA$_2$/PANI, one can see that it has completely different but homogenous structure consisting in straight or twisted

rods of polyaniline of about 40 nm diameter and ~200 nm length, an observation which is in line with exfoliation as deduced from XRD (see below). Interestingly, without any diazonium pretreatment, the B/PANI nanocomposite displays mixed regions from uncoated bentonite and PANI deposits. This uneven in situ deposition of PANI has an effect on the conductivity, a property which will be tackled below (see Section 3.7).

3.5. Transmission electron microscopy

TEM images for bentonite and its nanocomposites are displayed in Figure 8. A perfect layered structure is displayed for bentonite in Figure 8a. Upon polymerization of aniline in the presence of diazonium exchanged clay, the B-DPA$_{0.6}$/PANI nanocomposite exhibits an unusual twisted layered structure (Figure 8b). The visible layered regions are much less dense than those of the pristine bentonite, a fact which is in line with intercalation of the clay. The effect of diazonium and in-situ polymerization is exacerbated in the case of B-DPA$_{1.3}$/PANI nanocomposite (Figure 8c). Indeed, one can still see the layered structure but with much higher interlayer distance. For this reason, the layered regions displayed in Figure 8c look much less dense. It is to note that both B-DPA$_{0.6}$/PANI and B-DPA$_{1.3}$/PANI nanocomposites exhibit single PANI-wrapped nanosheets of bentonite (indicated by arrows). To finish, as shown in Figure 8d, the basal spacing of the nanocomposite B-DPA$_2$/PANI has drastically increased and has given rise to a different morphology which accounts for an onset of exfoliation. Indeed, as described 6 decades ago, Norrish[49] has set 4 nm as the nominal distance between lamellae for montmorillonite to become exfoliated. Oppositely, without any diazonium cation exchange pretreatment, the bentonite nanosheets remain very densely packed in the case of B/PANI nanocomposite (Figure 8e). The interlamellar distance is about 1.34 nm, matching the distance assessed by means of XRD (see Section 3.6).

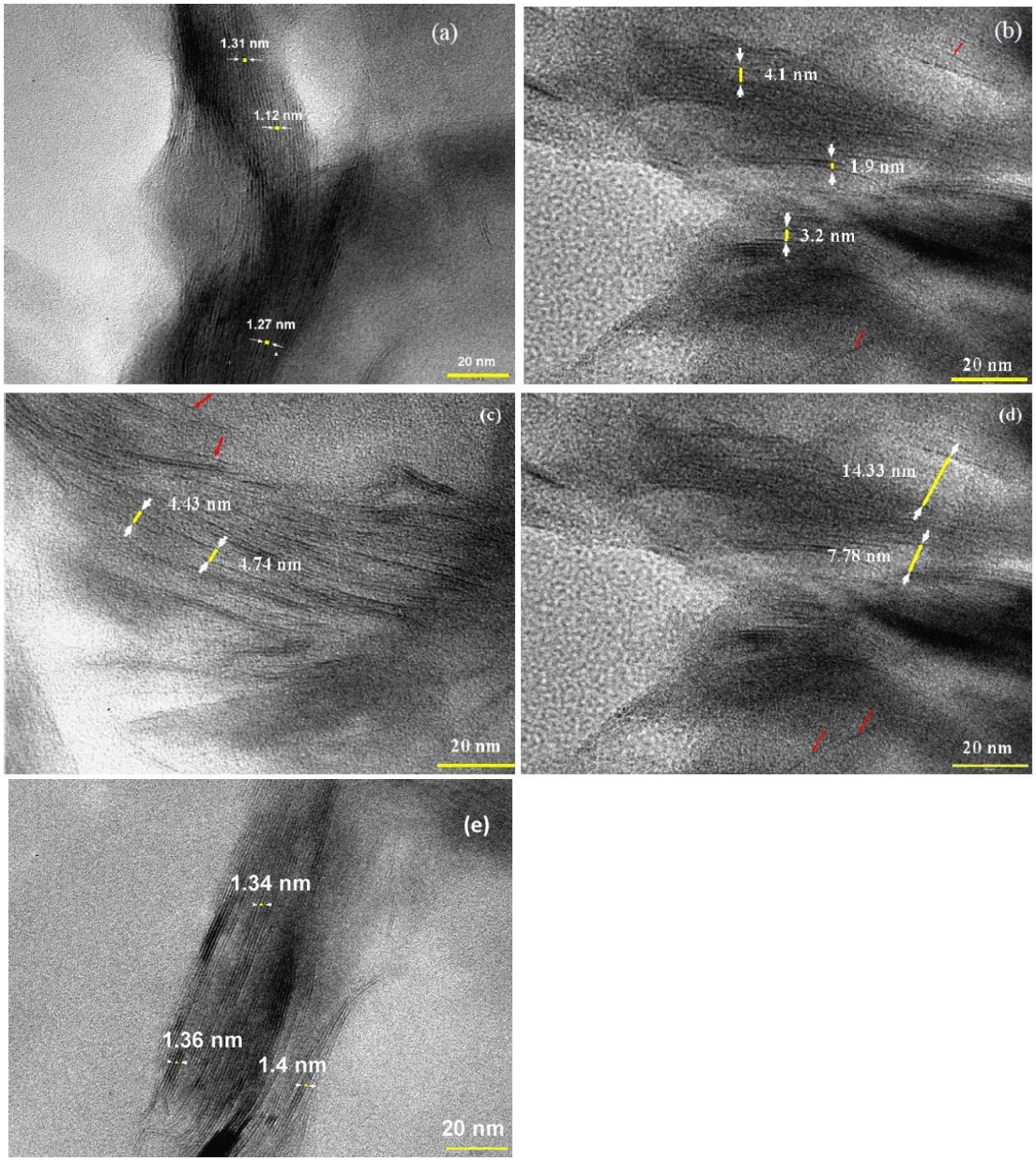

Figure 8. TEM images of (a) Bentonite, (b) B-DPA$_{0.6}$/PANI, (c) B-DPA$_{1.3}$/PANI, (d) B-DPA$_2$/PANI, and (e) B/PANI.

3.6. X-ray diffraction

The XRD patterns of bentonite, B-DPA$_2$ and its corresponding nanocomposite B-DPA$_2$/PANI are displayed in Figure 9. In order to determine the effect of diazonium cation

exchange on the X-ray diffraction properties, we also display the XRD pattern of B/PANI. Bentonite is characterized by a diffraction peak at $2\theta \approx 6.7°$ which shifts to lower angle after diazonium cation exchange before vanishing upon polymerization of aniline. Note that for bentonite and B-DPA_2, the peak at $2\theta \approx 50°$ is due to quartz impurity. After polymerization of aniline in the presence of diazonium cation exchanged clay, the XRD pattern of B-DPA_2/PANI completely lacks the diffraction peak of bentonite mentioned above, which suggests exfoliation or onset of exfoliation of the clay.

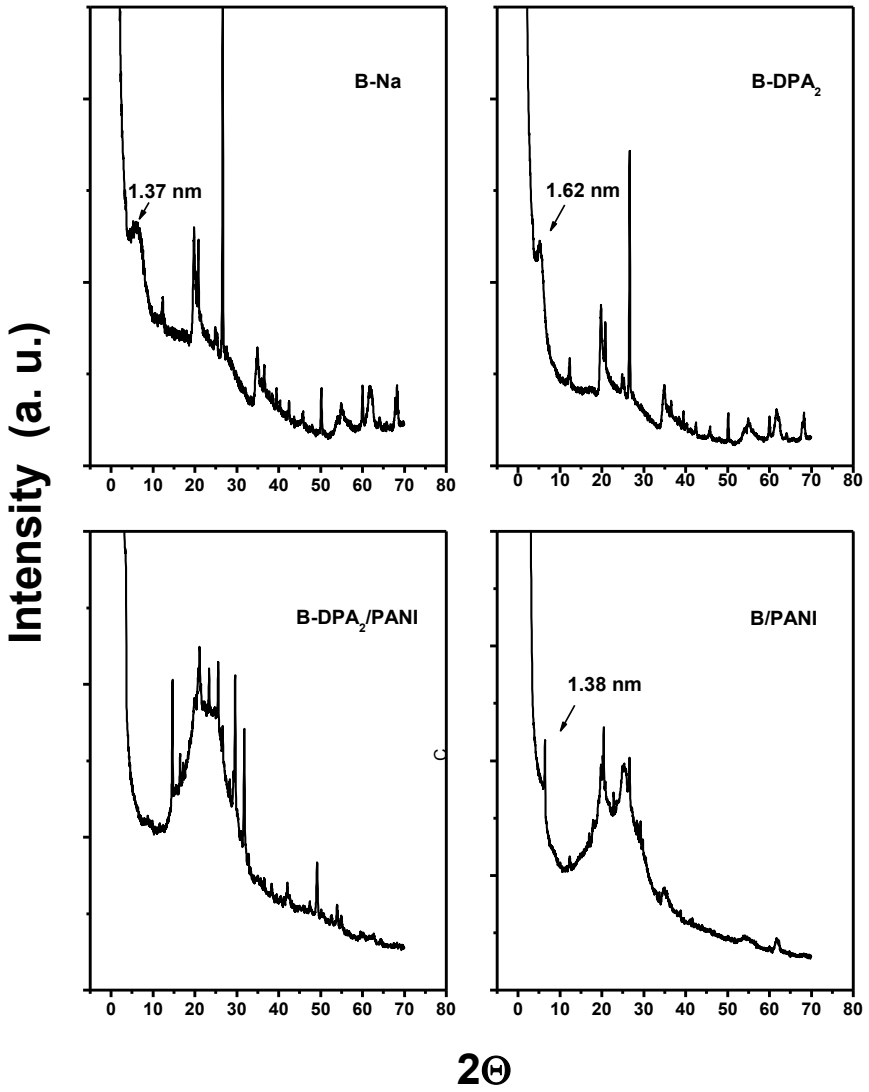

Figure 9. XRD patterns for bentonite, B-DPA_2, B-DPA_2/PANI and B/PANI samples.

The average interlamellar distance was estimated to be 13.7 and 16.2 Å for bentonite and B-DPA_2, respectively. As the nanocomposite BP-DPA_2/PANI exhibits only a broad diffraction pattern assigned to polyaniline, it was not possible to determine the interlamellar distance and the nanocomposite is most likely to be exfoliated or at least at a very high extent of intercalation. This corroborates the hypothesis of PANI grafting to the clay sheets. For the nano-hybrid, the broad peaks at ~ 19–20° and ~ 25–26° can be ascribed to the characteristic parallel and perpendicular periodicity of PANI chains.[50]

The XRD results obtained so far indicate clear differences in the crystalline structure of the nancomposites. Therefore, the diazonium exchange reaction is an important step towards the preparation of highly intercalated to exfoliated bentonite/PANI nanocomposites. Indeed, without any diazonium cation exchange pretreatment, B/PANI exhibits an X-ray diffraction peak at $2\theta \approx 6.7°$ corresponding to quasi the same interlamellar distance in pristine bentonite.

3.7. Electrical conductivity

The electrical conductivity of pure PANI, pristine bentonite, B-Na/PANI and the B-DPA$_x$/PANI nanocomposites were measured using the standard four probe method at room temperature (Table 2). For comparison, the preparation method, conductivity, morphology and potential applications of selected clay/PANI nanocomposites, designed elsewhere, are also reported in Table 2.

Table 2. Summary of preparation methods and electrical and morphological features of clay/PANI nanocomposites.

Clay	Surface modifier	Experimental details	Structure and conductivity	Application	Ref.s
Illite	-	Chemical polymerization of aniline with $(NH_4)_2S_2O_8$ (0·2 M) as oxidizing agent for (3–4 h) in ice-bath	Exfoliated illite/PANI nanocomposite (σ= 10^{-3} S/cm)	NA	51
Cloisite 30B nano-clay	methyl, tallow, bis-2-hydroxyethyl, quaternary ammonium chloride	Supercritical CO_2 was used as processing medium to prepare PANI/clay and self-doped PANI/clay nanocomposites. m-aminobenzenesulfonic acid and APS were the oxidants	Intercalated (σ= 2 S/cm for 5% w/w clay)	NA	52
Cloisite 15A	Dimethyl dihydrogentaed tallow ammonium chloride	aniline polymerization in 1.5 M HCl, APS as oxidant	Structure: NA (σ= 1.65 S/cm)	anticorrosive properties	53
MMT	modified-montmorillonite (Na-MMT, Cu-MMT or Fe-MMT)	dispersed in water using ultrasonication for 5 h. Then, 0.22 mol of aniline was added, followed addition of 1 M perchloric acid $HClO_4$. stirred for 24 h	clay intercalated structure (σ = 12.8x10^{-5} S/cm)	Conducting polymer _	54
MMT and vermiculite	-	anilinium hydrochloride and anilinium sulfate are used like dopent	Intercalated (in plane conductivity, $\sigma\|\|$ = 0.084 S/cm)	NA	55
Bentonite (B-Na)	-	Raw clay purified with sodium (Na)	(σ = 10^{-9} S/cm)	NA	This work
Polyaniline (PANI)	-	Oxidative polymerization of 0.16 mol aniline with 0.04 mol ammonium persulfate (APS)	σ=1 x 10^{-2} S/cm	NA	This work
B-Na/PANI	-	In situ polymerization of aniline in the presence of purified bentonite.	σ=2.1x10^{-8} S/cm	NA	This work
B-DPA$_{0.6}$ /PANI	4-diphenylamine diazonium salt (DPA)	Purified bentonite was first cationically exchanged at a CEC fraction of 0.6 of DPA, followed by the in-situ oxidative polymerization of 0.16 mol of aniline with 0.04 mol ammonium persulfate (APS)	σ=1.2 x10^{-4} S/cm	NA	This work
B-DPA $_{1.3}$/PANI	4-diphenylamine diazonium salt (DPA)	Same method as for B-DPA$_{0.6}$ /PANI except that DPA concentration was 1.3 CEC.	σ=8.2 x10^{-4} S/cm	NA	This work
B-DPA$_2$/PANI	4-diphenylamine diazonium salt (DPA)	Same method as for B-DPA$_{0.6}$ /PANI except that DPA concentration was 2 CEC.	σ=24 x10^{-4} S/cm	NA	This work

APS: $(NH_4)_2S_2O_8$; tallow: ~65% C18, ~30% C16; 5% C14; MMT: Montmorillonite; NA: not available;

First, the actual PANI has a conductivity matching that reported for an initial oxidant/aniline ratio of ~0.25.[56] Conductivity of PANI has actually been demonstrated to be stable for an oxidant/aniline ratio in the 0.25-1.15 range.[57] Concerning the nanocomposites, it is worth to note an increase in the conductivity of the nanocomposites with increasing extent of diazonium bentonite modification. Compared to unmodified clay, the diazonium cation exchange prior to polymerization imparts a quantum jump in the conductivity, *i.e.* up to 5 orders of magnitude. Interestingly, without any diazonium cation exchange B-Na/PANI has a conductivity of $2.1x10^{-8}$ S/cm, about 1 order of magnitude only higher than that of bentonite. For all nanocomposites made with diazonium-exchanged bentonite, the intercalation favours the loading of the conductive polymer which increases the electronic conductivity from $1.2x10^{-4}$ to $24x10^{-4}$ $S.cm^{-1}$ range. Similar values were obtained for PANI prepared in different inorganic hosts (PANI-MMT modified with sodium copper and iron conductivities ranging from $24.2x10^{-5}$ to $12.8x10^{-5}$ S cm^{-1}).[18] The conductive character of the B-DPA_x/PANI nanocomposites is most probably due to the intimate contact between single PANI-wrapped clay sheets. The PANI-PANI contact is thus at the origin of the conductive paths within the nanocomposites. One can thus argue that without any diazonium exchange process, stacked, and not single, clay sheets are wrapped by PANI (see TEM Figure 8e). Still, the best achieved conductivity (for B-DPA_2/PANI) remains lower than 1.65 S cm^{-1} obtained by Olad *et al*.[53] for a cloisite/PANi nanocomposite with 5 w/w% clay.

As far as other nanocomposites are concerned in Table 2, one can clearly see that the actual work provides for the first time a unique, novel diazonium cation exchange route for conductive, exfoliated clay/PANI nanocomposites.

Conclusion

Clay/polyaniline nanocomposites were prepared by in-situ oxidative polymerization of aniline in the presence of 4-diphenylamino diazonium-exchanged clay. The insertion of the diazonium and its reaction with clay was tracked by XPS and vibrational spectroscopies. XPS indicated a gradual change in the surface composition of clay with diazonium initial concentration. However, with either 0.6, 1.3 or 2 times the cation exchange capacity (CEC) of the clay the initial diazonium concentration induces the same surface composition which is PANI-rich for all nanocomposites. Suprisingly, without any diazonium salt pre-modification, the bentonite exhibits a PANI-rich surface however with an uneven deposition of the conductive polymer. As far as the morphology is concerned, it is demonstrated to be closely related to the diazonium exchange reaction prior to polymerization. PANI is evenly coated on cation exchanged bentonite but not the pristine clay. Diazonium cation exchange imparts high interlamellar spacing in the nanocomposites and a high exfoliation is reached for an initial concentration of the diazonium salt equal to 2 times the CEC. Of paramount importance for applications where there is a demand for conductive nanocomposites, the diazonium modification of clay induces a quantum jump in conductivity (up to 5 orders of magnitude) compared to pristine clay/PANI nanocomposite.

Beyond these results, we demonstrate for the first time that aryl diazonium salts are unique intercalants and coupling agents for conductive polymers to clay; they impart high conductivity and exfoliation to the end clay/PANI nanocomposites. This is achieved in a simple and efficient manner which is expected to open new horizons to the materials scientist.

Acknowledgements
K.J. wishes to thank Campus France for a provision of a scholarship within the framework of a Tunisian-French Co-tutelle PhD program. MMC and DKA are indebted to CEFIPRA/IFCEPAR for financial support (Project No 4705-2). The authors would like to thank Ms Sophie Nowak, Ms H. Lecoq and Mr L. Mouton for their assistance with XRD, SEM and TEM characterizations, respectively.

References

[1] *Aryl Diazonium Salts: New Coupling Agents in Polymer and Surface Science,* M. M. Chehimi (Ed.), © 2012 Wiley-VCH Verlag GmbH & Co. KGaA, Weinheim, Germany (ISBN: 978-3-527-32998-4).

[2] J. Pinson, F. Podvorica, *Chem. Soc. Rev.*, 2005, **34**, 429-439.

[3] D. Bélanger, J. Pinson, *Chem. Soc. Rev.*, 2011, **40**, 3995-4048.

[4] J. J. Gooding, S. Ciampi, *Chem. Soc. Rev*., 2011, **40**, 2704-2718.

[5] M. Delamar, R. Hitmi, J. Pinson, J. M. Savéant, *J. Am. Chem. Soc.*, 1992, **114**, 5883–5884.

[6] J. M. Tour, *J. Org. Chem.*, 2007, **72**, 7477–7496.

[7]J. Wang, M. A. Firestone, O. Auciello, J. A. Carlisle, *Langmuir*., 2004, **20**, 11450–11456.

[8] C. Mangeney, Z. Qin, S. A. Dahoumane, A. Adenier, F. Herbst, J.-P. Boudou, J. Pinson, M. M. Chehimi, *Diamond Relat. Mater.*, 2008, **17**, 1881–1887.

[9] Z. Salmi, A. Lamouri, P. Decorse, M. Jouini, A. Boussadi, J. Achard, A.Gicquel, S. Mahouche-Chergui, B. Carbonnier, M. M. Chehimi. *Diamond Relat. Mater*. 2013, **40**, 60-68.

[10] R. Hunger, W. Jaegermann, A. Merson, Y. Shapira, C. Pettenkofer, J. Rappich, *J. Phys. Chem. B.*, 2006, **110**, 15432–15441.

[11] D. K. Aswal, S. P. Koiry, B. Jousselme, S. K. Gupta, S. Palacin, J. V. Yakhmi, *Physica E,* 2009, **41**, 325–344.

[12] M. M. Chehimi, A. Lamouri, M. Picot, J. Pinson, *J. Mater. Chem. C.*, 2014, **2**, 356-363.

[13]V. Mévellec, S. Roussel, L. Tessier, J. Chancolon, M. Mayne-L'Hermite, G. Deniau, P. Viel, S. Palacin, *Chem. Mater*., 2007, **19**, 6323–6330.

[14] N. Griffete, R. Ahmad, H. Benmehdi, A. Lamouri, P. Decorse, C. Mangeney, *Colloids Surf. A: Physicochem. Eng. Asp.*, 2013, **439**, 145–150.

[15] Z. Salmi, S. Gam-Derouich, S. Mahouche-Chergui, M. Turmine, M. M. Chehimi, *Chem. Pap*., 2012, **66**, 369-391.

[16] A. Blacha, P. Koscielniak, M. Sitarz, J. Szuber, J. Zak, *Electrochim. Acta.*, 2012, **62**, 441–446.

[17] L. M. Santos, J. Ghilane, C. Fave, P. C. Lacaze, H. Randriamahazaka, L. M. Abrantes, J.-C. Lacroix, *J . Phys. Chem. C.,* 2008, **112**, 16103–16109.

[18] A. Mekki, S. Samanta, A. Singh, Z. Salmi, R. Mahmoud, M. M. Chehimi, D. K. Aswal, *J. Colloid Interface Sci.*, 2014, **418**, 185–192.

[19] H. A. Dabbagh, A. Teimouri, A. N. Chermahini, *Dyes Pigments*, 2007, **73**, 239–244.

[20] Z. Salmi, K. Benzarti, M. M. Chehimi, *Langmuir*, 2013, **29**, 13323–13328.

[21] M. G. Hosseini, M. Raghibi-Boroujeni, I. Ahadzadeh, R. Najjar, M. S. S. Dorraji, *Prog. Org. Coat*., 2009, **66**, 321–327.

[22] X. Lu, W. Zhang, C. Wang, T-C. Wen, Y. Wei , *Prog. Polym. Sci*., **36**, 671–712.

[23] K. Jlassi, A. Singh, D. K. Aswal, R. Losno, M. Benna-Zayani, M. M. Chehimi, *Colloids Surf. A Physicochem. Eng. Asp.*, 2013, **439**, 193–199.

[24] R. C. Silva, M. V. Sarmento, F. A. R. Nogueira, J. Tonholo, R. J. Mortimer, R. Faez, A. S. Ribeiro, *RSC Adv.*, 2014, **4**, 14948-14955.

[25] M. Omastová, M. Mičušík, *Chem. Pap*., 2012, **66**, 392-414.

[26] M. Mravčáková, K. Boukerma, M. Omastová, M. M. Chehimi, *Mater. Sci. Eng. C.*, 2006, **26**, 306–313.

[27] C. Perruchot, M. M. Chehimi, M. Delamar, F. Fievet, *Surf. Interface Anal.*, 1998, **26**, 689–698.

[28] C. Perruchot, M. M. Chehimi, M. Delamar, E. Cabet-Deliry, B. Miksa, S. Slomkowski, M. A. Khan, S. P. Armes, *Colloid Polym. Sci.*, 2000, **278**, 1139-1154.

[29] M. Benna, N. Kbir-Ariguib, C. Clinard, F. Bergaya, Prog. *Colloid. Polym.Sci*., 2002, **117,** 204-210.

[30] H.Othmani-Assmann, M. Benna-Zayani, S. Geiger, N.Kbir-Ariguib, M .Trabelsi-Ayadi, N. E. Ghermani, J. L. Grossiord, *J. Phys. Chem.C. ,* 2007,**111**, 10869-10877.

[31] P. T. Hang, G. W. Brindley, *Clays Clay Miner*. 1970, 18, 203-212.

[32] A. Di Gianni, E. Amerio, O. Monticelli, R. Bongiovanni, *Appl. Clay Sci*., 2008, **42**, 116–124.

[33] W. Boyle Jr., T. J. Broxton, J. F. Bunne, *Chem. Commun*. 1971, 1469-1470.

[34] G. Ćirić-Marjanović, *Synth. Met.*. 2013, **177**, 1–47.

[35] V. Orlov, S. Zh. Ozkan, G. P. Karpacheva, *Polym. Sci. Ser.B*, 2006, **48**, 11-17.

[36] B. Massoumi, Sh. Najafian, A. A. Entezami, *Polym. Sci. Ser.B*, 2010, **52**, 270-276.

[37] M. Trchová, Z. Morávková, I. Šeděnková, J. Stejskal, *Chem. Pap.*, 2012, **66**, 415-445.

[38] S. Caillère, S. Henin, M. Rautrureau (Eds.), *Minéralogie Des Argiles.*, 1982, Vols I and II, Masson, Paris (France).

[39] M. Trchová, Z. Morávková, I. Šeděnková, J. Stejskal, *Chem. Pap.*, 2012, **66**, 415-445.

[40] K. R. Reddy, B. C. Sin, K. S. Ryu, J. C. Kim, H. Chung, Y. Lee, *Synth. Met.*, 2009, **159,** 595-603.

[41] I. Sedenkova, J. Prokes, M. Trchova, J. Stejskal, *Polym. Degrad. Stab*., 2008, **93**, 2147–2157.

[42] R. Cruz-Silva, J. Romero-Garcı, J.L. Angulo-Sanchez, E. Flores-Loyola, M. H. Farıas, F.F. Castillon, J.A. Dıaz, *Polymer*, 2004, **45**, 4711-4717.

[43] M. Baibarac, I. Baltog, S. Frunza, A. Magrez, D. Schur, S.Yu. Zaginaichenko, *Diamond Relat. Mater.*, 2013, **32,** 72–82.

[44] E. Marie, R. Rothe, M. Antonietti, K. Landfester, *Macromolecules*, 2003, **36**, 3967–3973.

[45] R. C. Yu King, F. Roussel, J. F. Brun, C. Gors, *Synth. Met.*, 2012, **162** , 1348–1356.

[46] S. Quillard, G. Louarn, S. Lefrant, A. G. Macdiarmid, *Phys. Rev. B*, 1994, **50**, 12496–12508.

[47] J. E. Pereira da Silva, M. L. A. Temperini, S. I. Cordoba de Torresi, *Electrochim. Acta*, 1999, **44**, 1887–1891.

[48] K. Hinrichs, K. Roodenko, J. Rappich, M. M. Chehimi, J. Pinson, Analytical methods for the characterization of aryl layers. in *Aryl Diazonium Salts. New Coupling Agents in Polymer and Surface Science*, M. M. Chehimi, ed., Wiley-VCH, Weinheim, 2012 Chap. 4, pp. 71-101.

[49] K. Norrish. *Discuss. Faraday Soc.*, 1954, **18**, 120-134.

[50] J. Wanga, J. Wang , Z. Yang , Z. Wang , F. Zhang , S. Wang, *React. Funct. Polym*., 2008, 68, 1435–1440.

[51] N. Serivastava, Y. Singh, R. A. Singh, *Bull. Mater. Sci.*, 2011, 34, 635-638.

[52] E. Akbarinezhad, M. Ebrahimi, F. Sharif, *Synth. Met.*, 2012, **162**, 1879–1886.

[53] A. Olad, A. Rashidzadeh, *Prog. Org. Coat*., 2008, **62**, 293-298.

[54] A. Zehhaf, E. Morallon, A. Benyoucef, *J. Inorg. Organomet. Polym*., 2013, **23**, 1485-1491.

[55] J. Tokarský, L. Kulhánková, V. Stýskala, K. Mamulová Kutláková, L. Neuwirthová, V. Matějka, P. Čapková, *Appl. Clay Sci.*, 2013, **80**, 126–132.

[56] N. Gospodinova, L. Terlemezyan, P. Mokreva, K. Kossev, *Polymer*, 1993, **34**, 2434-2437.

[57] S. P. Armes, J. F. Miller, *Synth. Met*., 1988, **22**, 385-393.